

# Clouds at Barbados are representative of clouds across the trade wind regions in observations and climate models

Brian Medeiros<sup>a,1</sup> and Louise Nuijens<sup>b,2</sup>

<sup>a</sup>National Center for Atmospheric Research, Boulder, CO 80307; and <sup>b</sup>Max Planck Institute for Meteorology, 20146 Hamburg, Germany

Edited by Benjamin D. Santer, Lawrence Livermore National Laboratory, Livermore, CA, and approved April 21, 2016 (received for review October 30, 2015)

Trade wind regions cover most of the tropical oceans, and the prevailing cloud type is shallow cumulus. These small clouds are parameterized by climate models, and changes in their radiative effects strongly and directly contribute to the spread in estimates of climate sensitivity. This study investigates the structure and variability of these clouds in observations and climate models. The study builds upon recent detailed model evaluations using observations from the island of Barbados. Using a dynamical regimes framework, satellite and reanalysis products are used to compare the Barbados region and the broader tropics. It is shown that clouds in the Barbados region are similar to those across the trade wind regions, implying that observational findings from the Barbados Cloud Observatory are relevant to clouds across the tropics. The same methods are applied to climate models to evaluate the simulated clouds. The models generally capture the cloud radiative effect, but underestimate cloud cover and show an array of cloud vertical structures. Some models show strong biases in the environment of the Barbados region in summer, weakening the connection between the regional biases and those across the tropics. Even bearing that limitation in mind, it is shown that covariations of cloud and environmental properties in the models are inconsistent with observations. The models tend to misrepresent sensitivity to moisture variations and inversion characteristics. These model errors are likely connected to cloud feedback in climate projections, and highlight the importance of the representation of shallow cumulus convection.

trade wind clouds | climate models | shallow cumulus | Barbados

Is the cloud structure and variability observed at a single location over a long time representative of more general regimes of clouds? This is the conceit of long-term observational “super sites” but has rarely been evaluated (1, 2). This work focuses on clouds found in trade wind regions, which are mostly shallow cumulus, and asks whether findings from the Barbados Cloud Observatory (BCO) are generalizable to the broader tropics in observations and climate models. We will evaluate cloud properties and the environment in which the clouds form across 12 climate models within these regions. This emphasis on the trades is motivated by several factors: (i) Previous studies suggest these are the regions that lead to much of the spread in estimates of climate sensitivity (3, 4), (ii) there is a dearth of evaluation of shallow cumulus in climate models (5), and (iii) space-based and ground-based observations of the trades have recently become available (6–8). This focus on trade wind regions is unique but builds upon previous, broader model evaluations that have, among other things, shown improvements in near-global cloud properties in the latest generation of climate models (9) and provided an overview of the vertical structure of cloud fraction (CF) and cloud water content over tropical oceans (10). Ref. 11 explores low-level, tropical clouds in climate models and separates shallow cumulus and stratocumulus regimes; that study reports compensating biases between cloud cover (CC) and radiative properties. Ref. 12 provides a detailed, process-oriented multiclimatic model evaluation of the covariability of clouds and environmental conditions at

a single location in the Atlantic trade wind region. A key result of that work is that the climate models’ low-level clouds are more susceptible to variations in the environment than observations indicate, and factors that are important for cloudiness in models are different from those in observations. The present study tests whether those findings can be generalized to the broader tropical oceans, and emphasizes the links between clouds and their radiative effects to the circulation.

To illustrate the association between clouds and the large-scale circulation, Fig. 1 shows the global and seasonal distributions of the cloud radiative effect (CRE, the difference in clear-sky and all-sky radiative fluxes at the top of the atmosphere) and midtropospheric vertical motion ( $\omega_{500}$ ) using satellite estimates [Clouds and the Earth’s Radiant Energy System, Energy Balanced and Filled (CERES EBAF) v2.8 (13)] and reanalysis [European Centre for Medium-Range Weather Forecasts Reanalysis (ERA)-Interim (14)]. (Table 1 lists the observational data sets used in this study.) Typical trade wind conditions exist under weak ascent to moderate subsidence ( $-15$ – $28$  hPa·d<sup>-1</sup> is the range used below) and show weak, negative CRE that corresponds to a slight cooling influence on the climate system. Trade wind regions are widespread and relatively constant; they do not show much seasonality in CRE, and vast swaths of the tropical oceans are characterized as trade wind regions throughout the year. The relative constancy of CRE across the trades differs from other regions. The midlatitude storm tracks, for example, have strong seasonality in CRE: Summertime storm tracks exhibit the strongest negative CRE. The quasi-permanent subtropical stratocumulus decks, on the other hand, exist under moderate to strong subsidence and also have strong negative CRE

## Significance

This paper shows that clouds near Barbados exhibit similar properties to those over much of the tropical oceans. This finding allows observations taken at Barbados to be generalized to the broader tropics. The same approach is applied to climate models to show that errors in simulated clouds near Barbados are similar to errors across the tropical oceans. The errors are related to the representation of the vertical structure of clouds and the boundary layer and the underlying turbulent and convective mixing that create the clouds. Because trade wind clouds are a key contribution to the spread in climate model estimates of climate sensitivity, improvements in these clouds could reduce uncertainty in climate projections.

Author contributions: B.M. and L.N. designed research, performed research, analyzed data, and wrote the paper.

The authors declare no conflict of interest.

This article is a PNAS Direct Submission.

Freely available online through the PNAS open access option.

<sup>1</sup>To whom correspondence should be addressed. Email: brianpm@ucar.edu.

<sup>2</sup>Present address: Department of Earth, Atmospheric and Planetary Sciences, Massachusetts Institute of Technology, Cambridge, MA 02139-4307.

This article contains supporting information online at [www.pnas.org/lookup/suppl/doi:10.1073/pnas.1521494113/-DCSupplemental](http://www.pnas.org/lookup/suppl/doi:10.1073/pnas.1521494113/-DCSupplemental).

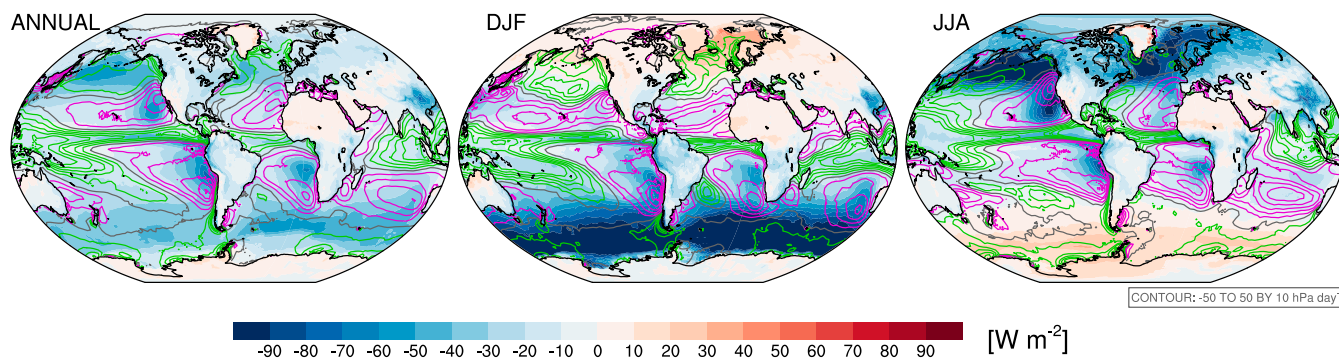


**Fig. 1.** Net CRE (watts per square meter) from CERES (March 2000 through December 2013) and 500-hPa vertical velocity ( $\omega_{500}$ , hectopascals per day) from ERA-Interim (January 1979 through December 2012). (Left) Annual average followed by the (Middle) December–February (DJF) and (Right) June–August (JJA) averages. Green contours indicate upward motion, and magenta contours denote downward motion. Contour lines are not included over land areas because the field becomes noisy.

(similar to the annual average CRE of the storm tracks), but cover a relatively small area that varies seasonally; as the stratocumulus decks recede toward the continents, trade wind regions expand. Regions with frequent deep convection (e.g., the Intertropical Convergence Zone) have relatively weak CRE because upper-level clouds have strong but nearly canceling shortwave (SW) and longwave (LW) CRE [CRE = SWCRE + LWCRE (15)], and many of these regions undergo large seasonal migrations that typically leave trade wind conditions in their absence.

Fig. 2 shows the climatological distribution of CRE and CC and their components over the tropical oceans (35°S–35°N) organized by using  $\omega_{500}$  to define dynamical regimes (16). Comparing the LWCRE with the long-term International Satellite Cloud Climatology Project [ISCCP (17)] CC estimate shows that strongly convective regimes have the most high-level cloud and correspondingly the strongest LWCRE. Like previous analyses (15), Fig. 2 shows strong compensation between the SW and LW CRE components in these regimes. The ISCCP CC estimates shown in Fig. 2 suggest little low-level CC in the convective regimes (around 5–10%) increasing to around 30% in the moderate to strong subsidence regimes. There is, however, substantial low-level cloud in the convective regimes, but it is obscured by higher cloud; evidence for this includes estimates that show ubiquitous low-level diabatic heating across the tropics (18). Deep convection is suppressed in the dry subsidence zones of the subtropics, so low-level clouds dominate these broad regions. The SWCRE of low-level clouds is weaker than that for upper-level clouds, but there is almost no LW compensation, so the SWCRE is dominant and provides a substantial cooling effect in the present climate (19, 20). The net CRE shows fairly large variability across dynamical regimes (gray shading), mostly dominated by the SW component, even in trade wind regimes with weak vertical motion. Although this variability seems at odds with the above discussion of the constancy of the trades, it is important to note that Fig. 2 shows variability within dynamical regimes, and so includes both spatial and temporal variability, including months that capture transitions in the large-scale circulation (all of which increase the variance).

**Table 1.** Data sets used in this study

Name	Interval	Fields	References
CALIPSO	2006–2014	CF, CC	(22)
CERES	2000–2013	CRE	(13)
ERA-Interim	1979–2012	$\omega$ , RH, T	(14)
ISCCP	1983–2008	CC	(17)
MISR	2000–2009	CC	(62)
MODIS	2002–2011	CC	(63)

$\omega$ , vertical pressure velocity; RH, relative humidity; T, temperature.

Also shown in Fig. 2 are the values for the Barbados region (defined as 300.5°E–305.5°E, 10.5°N–15.5°N, similar to ref. 21) separated by season. In each season, the Barbados region lies within the  $\pm 1\sigma$  envelope of the broader tropical oceans. This supports the idea that Barbados is a weakly convective environment during the summer wet season and a moderately subsiding one in the winter dry season (8), and the cloud properties within each season are similar to other such environments. To make use of this seasonal variation, we define the weak convection and moderate subsidence regimes roughly centered on the mean seasonal values of  $\omega_{500}$  in the Barbados region: The weak convection regime is defined as  $-15 \leq \omega_{500} \leq -5 \text{ hPa} \cdot \text{d}^{-1}$ , and the moderate subsidence regime will be defined by  $18 \leq \omega_{500} \leq 28 \text{ hPa} \cdot \text{d}^{-1}$ . Results presented herein are not very sensitive to these ranges.

Orbiting active remote sensing instruments provide insights into the vertical distribution of clouds over much more extensive areas and longer times than was previously possible. An example of this enhanced data coverage, Fig. 3, presents CF derived from Cloud-Aerosol Lidar and Infrared Pathfinder Satellite Observations (CALIPSO) measurements over the tropical oceans for June 2006 through December 2012 using the GCM-Oriented CALIPSO Cloud Product (CALIPSO-GOCCP) (22) composited using  $\omega_{500}$  from ERA-Interim (Table 1). As in Fig. 2, monthly data have been averaged in ranges of  $\omega_{500}$  to separate dynamical regimes. The close relationship between clouds and circulation emerges, with high clouds being focused in convective regimes and low-level clouds predominant in subsiding regimes. It is important to note, however, that high-level and low-level clouds frequently cooccur, including in the trade wind regions, and can be thermodynamically linked (through local convection) or not (23). Also shown in Fig. 3 are the profiles of CF in the Barbados region during the summer and winter months, and, as seen above, the profiles show the clouds differ with season in the Barbados region as the regional circulation changes. In both seasons, there are frequent low-level clouds with maxima near the lifted condensation level (LCL) and higher up near the trade inversion (6, 24). The dotted lines in Fig. 3, Right show the profiles from the dynamical regimes that the Barbados region falls into in summer and winter. The similarity is clear. The main difference is in winter, when the moderate subsidence regime has a unimodal low-level cloud layer that is cloudier than the Barbados region; this is because the regime samples a variety of thermodynamic states that support clouds varying from nearly overcast conditions associated with stratiform outflow layers and cumulus under stratocumulus to fields of isolated trade wind cumulus. Here we accept this variability within the dynamical regime with the knowledge that cloud types within subsidence regimes can be more readily discerned when sorted by a thermodynamic variable such as lower-tropospheric stability (25) or sea surface temperature (SST) (26).

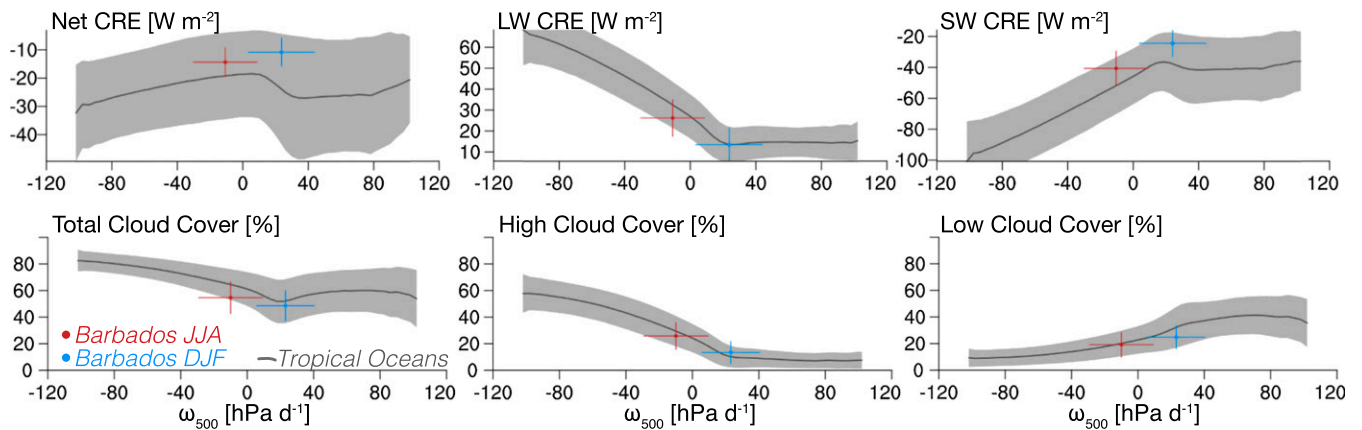


**Fig. 2.** Cloud properties sorted into dynamical regimes using  $\omega_{500}$  (horizontal axis). The  $\omega_{500}$  is taken from ERA-Interim monthly means. (Upper) CRE, LWCRE, and SWCRE from CERES EBAF v2.8 and (Lower) total, high, and low CC from ISCCP. The ERA-Interim  $\omega_{500}$  is regridded to match the cloud properties horizontal grids; the temporal period is the overlapping time between each data source. The solid gray lines show the area-weighted average in  $\omega_{500}$  bins over the tropical oceans ( $\pm 35^\circ$  latitude), and the gray shading shows the area-weighted SD within each bin. The markers show the values in the  $5^\circ$  box upstream of Barbados, with the lines showing the SD in each quantity. The red is the JJA season, and the blue is the DJF season, both using the same temporal range as the full tropical calculation.

Taken together, Figs. 1–3 provide context for understanding the distribution of clouds over tropical oceans, the connection between clouds and circulation, and their radiative impacts on the present climate. They also suggest that clouds observed at the BCO are representative of common tropical cloud regimes. Throughout the remainder of this study, we investigate whether climate models reproduce the observed clouds, the environments in which the clouds form, and the relationships between clouds and the environment.

### Climate Models

As discussed in the Introduction, the low-level clouds of the weak ascent to moderate subsidence regimes are primarily responsible for the spread in estimates of cloud feedback (and therefore climate sensitivity) among climate models. For a model's future climate projection to be credible, a necessary (but insufficient) condition is an adequate representation of cloud properties in the

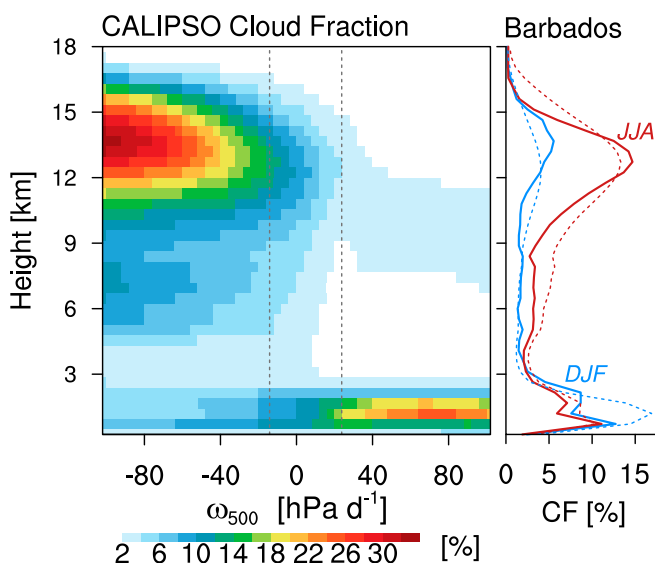
current climate. Previous work has shown that, in the weakly convecting to moderately subsiding regimes, there is reasonable agreement in CRE among the models (3), with values similar to the observed CRE in Fig. 2. Both total and low-level CC are generally underestimated by the models, however, leading to a “too-few-too-bright” problem in most climate models (11). The spread among the models' CRE is greatest in the strongly convecting regimes that cover only a small fraction of the tropics (3), but small biases in the more common trade wind regimes dominate any global bias.

To investigate trade wind clouds in climate models, we use a subset of the “AMIP” simulations available as part of the Coupled Model Intercomparison Project Phase 5 (CMIP5) (see Table S1 for the list of models). These are global simulations of the atmosphere and land surface forced by observed SST, sea ice cover, and greenhouse gas concentrations. Using observed SST removes important feedbacks between the surface temperature and atmosphere, but removes the SST biases that atmosphere–ocean global climate models (GCMs) consistently produce [for example, in the western Atlantic near Barbados (27, 28)]. The AMIP framework provides a test of the atmospheric component of climate models given a realistic SST distribution. Monthly average output is used during the interval 1979–2005; using monthly mean output limits some interpretation of relationships between clouds and their environment because much of the variance is associated with faster timescales (12, 24).

Model selection is based on the availability of output, especially satellite simulator output that is used to quantify CC [total (CC), high ( $CC_{HI}$ ), and low ( $CC_{LO}$ )] and CF. CF is here taken to be a measure of cloud within a grid cell; therefore, CF has a vertical distribution, and CC is the vertical integral of CF using assumptions about how partially cloudy layers overlap. That is, CC is the geometric projection of clouds onto the surface. Low-level CC,  $CC_{LO}$ , is typically defined for the layer from 680 hPa ( $\sim 3$  km) to the surface. Satellite simulators “observe” the simulated atmosphere in a similar manner to how the corresponding satellites observe the real atmosphere, allowing a direct comparison between models and observations (29). The simulated CRE is derived from the top-of-atmosphere radiative fluxes; the mean  $\omega_{500}$  and CRE are qualitatively reproduced by all of the models (Fig. S1), although every model shows errors in the details of the circulation, cloud pattern, and seasonality.

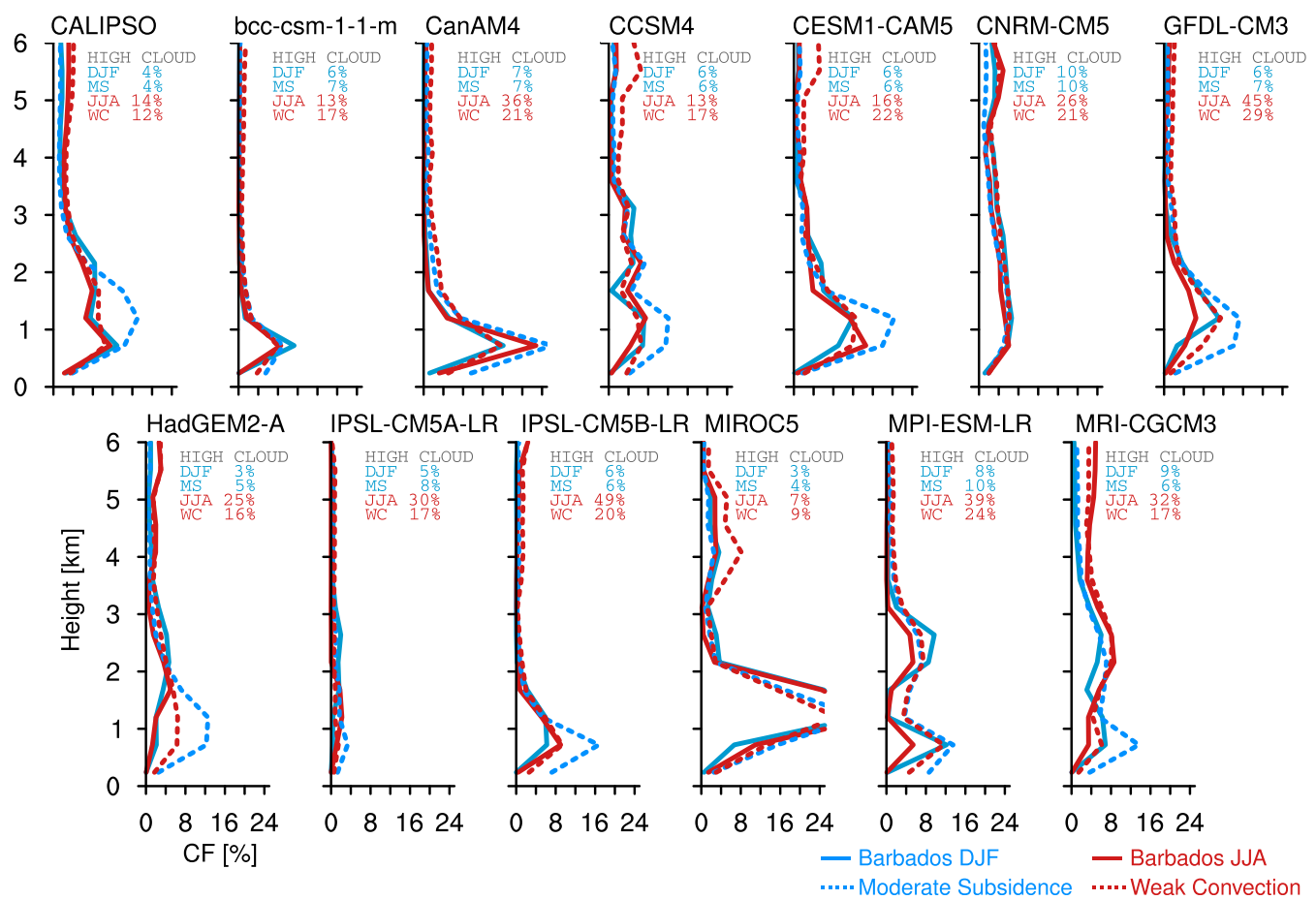
### Trade Wind Clouds and Their Environment

Fig. 4 shows the CF profiles for each model using their CALIPSO simulators. These profiles can be compared directly to those in



**Fig. 3.** (Left) CALIPSO CF averaged conditionally in bins of ERA-Interim  $\omega_{500}$  over the tropical oceans. (Right) CALIPSO CF averaged over the Barbados region for DJF (blue solid line) and JJA (red solid line). Dotted vertical lines mark the Barbados region's regime in each season (Left) and the regime profile for comparison with the seasonal profiles (Right).





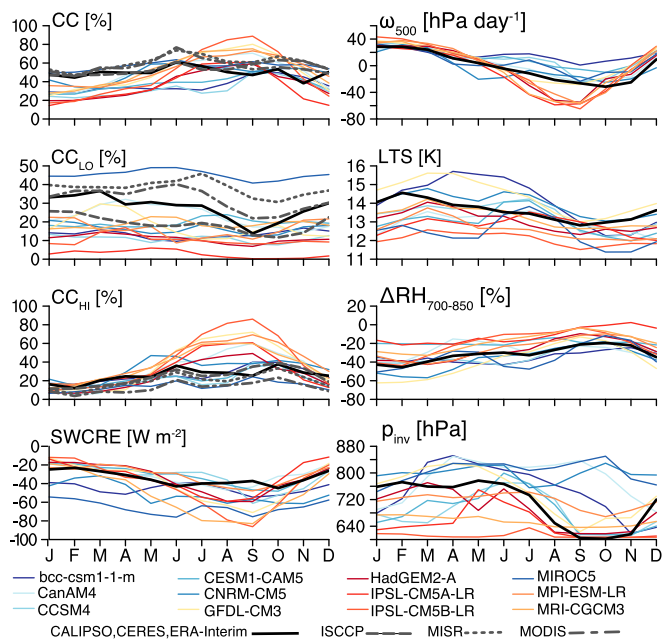
**Fig. 4.** CF profiles for CALIPSO (Upper Left) and each model derived from the CALIPSO simulator output. As in Fig. 3, dark, solid lines show the Barbados region in DJF (blue) and JJA (red), and dotted lines show the corresponding regime composites. High-level cloud, defined as the maximum CF above 8 km, is reported for each sampling strategy (MS stands for moderate subsidence, and WC stands for weak convection, as defined in the Introduction).

Fig. 3, but Fig. 4 focuses on the lower troposphere, where shallow convective clouds manifest very differently among the models. Inspection of the low-cloud distribution shows a variety of shapes of the cloud profile, including some models that form a shallow, unimodal distribution and others with a bimodal distribution. Observations and models both show modest seasonal variation in the low-level cloud. There is good correspondence between the cloud structure near Barbados and the  $\omega_{500}$ -based regimes. Several models produce a cloudier low-level cloud layer in the moderate subsidence regime than the Barbados region, consistent with the observations, but none capture the distinct difference in shape shown in the observations. Some models also have the moderate subsidence regime peak CF at a lower altitude, indicating a shallower boundary layer and more stratocumulus-like clouds in the regime compared with the shallow cumulus expected near Barbados. The model climatologies capture the observed slightly bottom-heavy cloud layer (using the metric of ref. 30), but the shape of the monthly mean profiles does not reflect the shape of instantaneous or even daily mean profiles (12).

The models also have biases in high-level clouds, which can be discerned using the maximum CF above 8 km (shown on Fig. 4). The height of this CF maximum is related to the model's upper tropospheric humidity (31) and varies from about 10 km to 14 km in these simulations. As with the low-level clouds, there is diversity in the simulated high-level clouds, but eight of the models produce more high cloud in the summer than CALIPSO (one produces too little). The models are more successful with the high cloud in winter, when there is large-scale subsidence and

little upper-level cloud. Although ERA-Interim  $\omega_{500}$  shows that the Barbados region transitions from moderate subsidence in the winter to weak convection in the summer (Fig. 3), it is not clear from Fig. 4 whether models correctly capture that feature of the large-scale circulation, and the biases in high clouds hint that the large-scale circulation could be misrepresented in some models.

Fig. 5 illustrates the clouds and environment of the Barbados region over the annual cycle for observations and models. As expected based on Fig. 4, most of the models overestimate the seasonality of  $CC_{HI}$  by producing too much high cloud in the summer. This seasonal variability of  $CC_{HI}$  is tied to the large-scale circulation, evidenced by an anticorrelation with  $\omega_{500}$ . Models that are overly convective during the summer are shown in red hues, and models that are not convective enough (compared with ERA-Interim) are in blues. All six models shown in red hues strongly overestimate the summertime high-cloud cover (as well as two of those shown in blue). This association of high clouds with circulation leads to a large spread of CC during the summer and a general overestimation of the amplitude of the annual cycle of CC. By contrast, low-level clouds provide an omnipresent background in both the models and satellite estimates that anchor the mean SWCRE but are generally underestimated by the models. The wintertime SWCRE (dominated by low-level clouds) is similar to the CERES estimate for many models even though CC and  $CC_{LO}$  are underestimated, but most of the models have an overly strong SWCRE in the summer, when  $CC_{HI}$  is overestimated. This finding is consistent with previous analyses that climate models have compensating biases in the low-cloud cover and cloud optical properties over tropical oceans (11).



**Fig. 5.** Composite annual cycle for the Barbados region using all available years. Climate models are shown by colors, and satellite or reanalysis are black and gray. The coloring of the models is based on the vertical velocity in the warm season, with warm hues used for models that are more convective than ERA-Interim and cool hues used for those that are less convective (the scale is otherwise arbitrary). (Left) Cloud characteristics (total CC, low-cloud cover, high-cloud cover, and shortwave CRE, from top to bottom) and (Right) environmental parameters (midtropospheric vertical pressure velocity ( $\omega_{500}$ ), lower-tropospheric stability, relative humidity difference between 700 hPa and 850 hPa, and inversion pressure level, from top to bottom).

Although high clouds are connected to the large-scale circulation, it is less clear what environmental factors control low-level clouds. Many studies have addressed the issue of cloud-controlling factors in observations (32–34) and models (35, 36). Most such studies have focused on stratocumulus clouds, and the consensus points toward a few primary controlling factors in that regime, including SST, subsidence, inversion strength (measured by lower-tropospheric stability,  $LTS = \theta_{700} - \theta_{stc}$ , or similar, where  $\theta$  is potential temperature), and humidity structure (37). In the trade wind regime, the controlling factors are unsettled because the boundary layer is a more complicated four-layer (dry convective subcloud, stable transition, conditionally unstable cloud, and stable inversion) structure (38, 39). Compared with stratocumulus regimes, the inversion is relatively weak, subsidence is more variable, and the strength and vertical structure of low-level winds can also be important (40).

Fig. 5 shows some of these factors for the annual cycle near Barbados. Relationships between  $CC_{Lo}$  and the environment vary across models; no robust low-cloud-controlling parameter emerges in the models. Fig. 5 exposes the annual cycle, but correlations between  $CC_{Lo}$  and the same environmental factors also show that there is no single factor that controls the low clouds, and models do not capture the same relationships between clouds and the environment as the observations and reanalysis (Fig. S2). The environmental factors shown in Fig. 5 do suggest, however, that the models are producing a broad array of boundary layer structures in the Barbados region. Inversion strength, lower-tropospheric convective mixing [measured by  $\Delta RH_{700-850}$ , the relative humidity difference between the free troposphere and the cloud layer (41)], and inversion level ( $p_{inv}$ , the pressure at the model level with maximum vertical gradient of liquid water potential temperature,  $d\theta/dp$ ) all vary substantially across the models, but do

not stratify the models like  $\omega_{500}$  in summer. Compared with ERA-Interim, the models tend to have weaker, higher inversions and stronger convective mixing (i.e.,  $\Delta RH_{700-850}$  closer to zero).

Observations suggest that cloud properties are generally similar between the Barbados region and the moderate subsidence regime (Fig. 2), although Barbados is slightly less cloudy, on average, than the broader regime. Fig. 5 shows that models tend to underestimate the total cloudiness in winter near Barbados, and that is nearly entirely due to underestimating the low-cloud cover. Fig. 6 expands to the broader regime and shows that climate models underestimate CC in moderate subsidence regimes, and they do so because of a low bias in  $CC_{Lo}$ . That is, the biases diagnosed near Barbados are similar to biases across the tropical oceans. The smaller  $CC_{Lo}$  near Barbados is consistent with the region being in the warmer, downstream portion of the regime and dominated by shallow cumulus with CC near 30% (6), whereas the regime also contains larger CC associated with stratocumulus and transitional clouds (25, 42). In contrast to the CC, the CRE is mostly well captured by the models (SWCRE is shown in Fig. 6; LWCRE is relatively small).

The models produce similar moderate subsidence environments to the reanalysis, but, as was found for the Barbados region, LTS and  $p_{inv}$  are underestimated by most models, indicating that the models are more convective than ERA-Interim (Fig. 6). Near-surface temperature (nominally at 2 m) is similar to ERA-Interim, as expected because it is constrained by the prescribed SST, so the bias in LTS can be associated with a low bias in  $\theta_{700}$ . This LTS bias also occurs in the Barbados region, which has a warmer SST than most locations within the regime. Although one might guess that inversion strength would constrain the humidity structure, the LTS bias does not appear to predict the cloud layer relative humidity ( $RH_{850}$ ) nor the convective mixing biases. The Barbados region is similar, in this regard, to the regime, but with a slightly higher mean  $RH_{850}$ . It appears that most climate models are producing a deeper trade wind boundary layer than expected, which could partly explain the underestimate of  $CC_{Lo}$  if the deeper, more convective layer acts to dry the lower levels and evaporate cloud. The relative humidity structures do not clearly indicate whether this is the case or not, but, because each model's cloud physics differ, it cannot be ruled out. That these biases occur for both the Barbados region, which is dominated by shallow cumulus, and the moderate subsidence regime, with its mixture of cloud types, suggests a systematic bias in boundary layer structure that is unlikely to be strongly associated with the large-scale circulation.

Fig. 7 repeats the same analysis, but switching to the weak convection regime and Barbados' summertime. Both the region and regime have near-surface temperatures about 2 K warmer than their counterparts in Fig. 6, and this warmer environment is associated with weaker LTS, a more humid cloud layer, and enhanced CC. The greater CC comes from both high- and low-level clouds, and the cloudier conditions reflect more sunlight producing a stronger SWCRE. Unlike the wintertime, some models show a significantly different  $\omega_{500}$  value than the observations for the Barbados region (Fig. 5). Those models are apparent in Fig. 7 by their low-biased LTS: They are more convective, as previously inferred. The remaining models, however, fail to capture the weaker stability in the summer, including all of the models with weak summertime  $\omega_{500}$  (blue in Fig. 5); those models misrepresent the seasonal pattern of the inversion by producing a lower, stronger inversion during summer. This bias is regional, however, as all of the models correctly produce higher, weaker inversions in the weak convection regime (see also Tables S1 and S2). Similarly, the high-level CC in the Barbados region is overestimated by most of the models (as seen in Fig. 4), but, across the weak convection regime, this is not the case. This shows that local circulation can be an important regional factor in weakly convective environments. Not all of the models would even classify the Barbados region in summer within the weak convection category, underscoring the role of local circulation biases for making comparisons with observations. Under

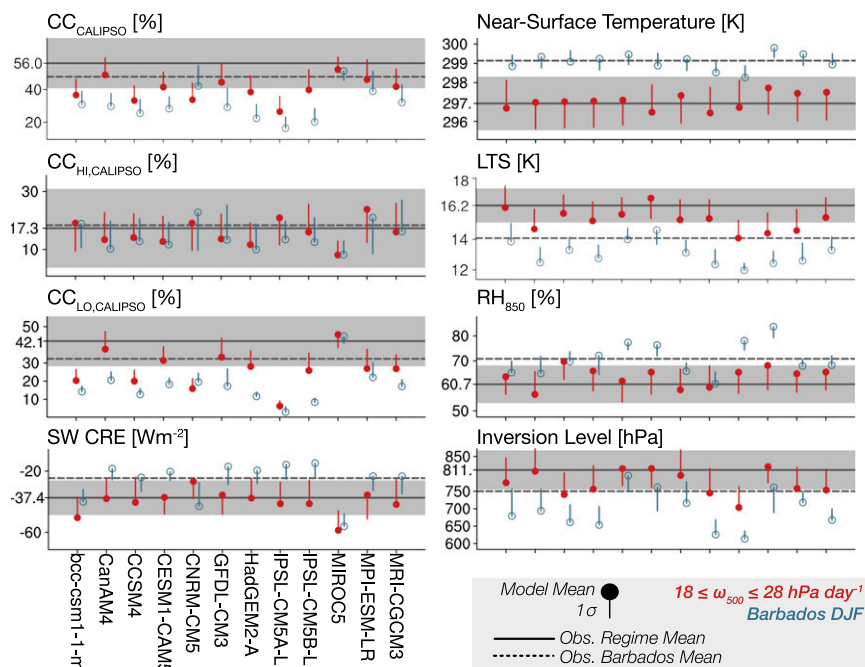


**Fig. 6.** Quantities averaged over the moderate subsidence regime (red) and in the Barbados region during DJF (blue) for the models. Horizontal lines show the observed values: solid for the regime, dashed for the region. Gray shading shows  $\pm 1\sigma$  for the observations in the regime; the stems show  $1\sigma$  for the models, directed to indicate the bias. The values for the regime are tabulated in [Table S1](#).

such circumstances, it may be more useful to construct composites from the site or region in the same manner as for the broader tropics and compare the frequency and structure of the conditionally sampled data (1); we have not included such an analysis.

Although Figs. 6 and 7 demonstrate the similarity between the mean, variability, and biases for the Barbados region and the dynamical regimes, quantitatively assessing the relationship

between the low-level cloud and the environment proves elusive. Fig. 8 provides a view into the complexity of the problem. The figure presents the correlation coefficients between  $CC_{LO}$  and four environmental factors thought to be related to the CC (and shown above); the correlations for the Barbados region are shown on the vertical axis, and the regimes are along the horizontal. Deviations from the 1:1 line show that the Barbados

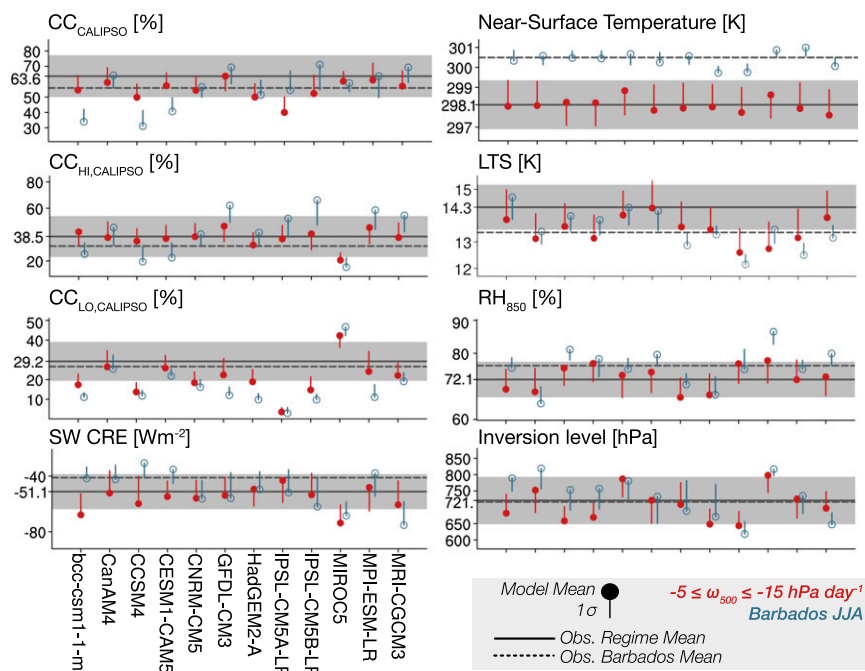


**Fig. 7.** As in Fig. 6, but for JJA in the Barbados region and for the weak convection regime defined as  $-15 \leq \omega_{500} \leq -5 \text{ hPa day}^{-1}$ . The values for the regime are tabulated in [Table S2](#).

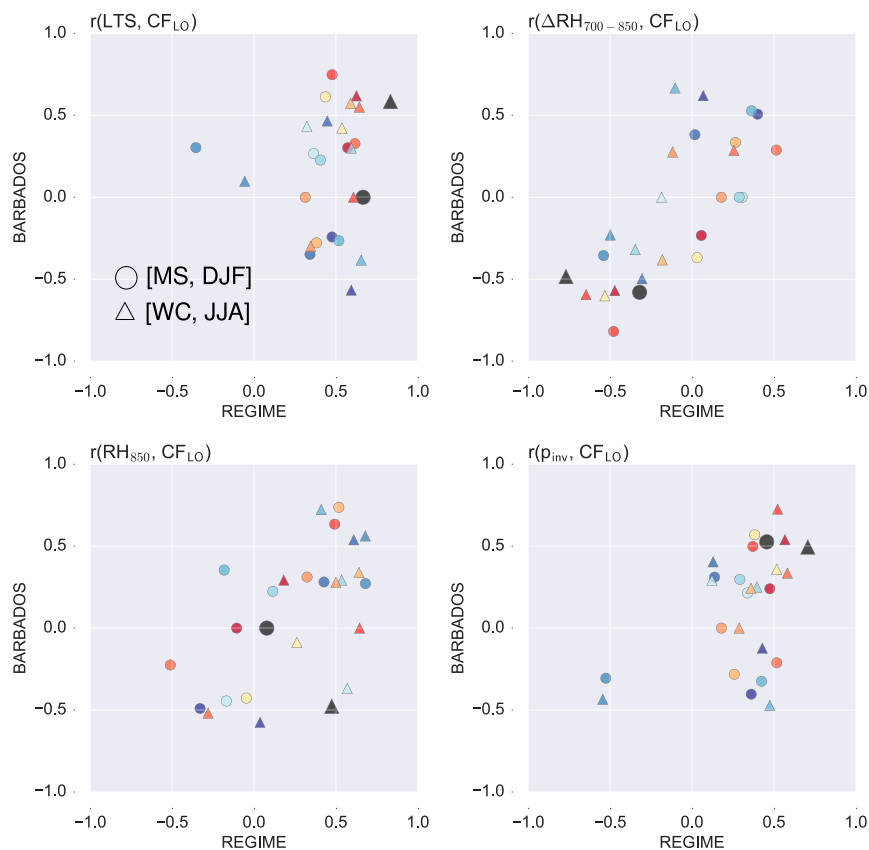


**Fig. 8.** Correlation coefficients between  $\text{CC}_{\text{LO}}$  and environmental parameters. The Barbados region is shown on the vertical, and the dynamical regime is shown on the horizontal. Circles denote the moderate subsidence and DJF sampling, and triangles show weak convection and JJA. Colors are as in Fig. 5. The values are derived by calculating the correlation coefficient at each spatial point using the monthly means, removing correlations that are not significant at the 95% level using a two-tailed  $t$  test, transforming the remaining coefficients using the Fisher  $z$  transformation, averaging the corresponding  $z$  values, and transforming that average back to correlation coefficient. This procedure provides an appropriate average correlation coefficient (61). The result of the significance test is to increase the resulting correlation coefficients, as insignificant correlations tend to be close to zero; there are a few instances where no correlations passed the significance test, and, in those cases, the coefficient is set to zero.

region imperfectly captures the relationships found in the broader regimes, but most of the correlations agree, at least in sign, between the region and regime. The discrepancies in this regard may indicate that the Barbados region is not representative of the regime, that it reflects only a subset of the regime, or that there could be confounding factors influencing the correlations. The tendency, however, is for the relationships to have the same sign and to be statistically significant in both the region and the regime, supporting the idea that clouds at a given site are similar to larger samples of clouds.

The troubling aspect of Fig. 8 is the diversity shown among the models and the dissimilarity from the observed linear relationships (larger, dark gray symbols). There are uncertainties associated with the observations: The reanalysis relies on data assimilation combined with a model (similar to other GCMs), both of which are subject to uncertainties and biases; similarly, the satellite observations are the result of limited sampling and retrieval algorithms that both introduce sources of error. The spread of the model relationships, regardless of the verisimilitude of the observational estimates, indicates that the models achieve their  $\text{CC}_{\text{LO}}$  through different balances of processes. These balances are likely to be internally consistent, but might not be a good representation of the real atmosphere. In some cases, the models do not capture the sign of the expected linear relationships. For example,  $\text{CC}_{\text{LO}}$  is expected to increase with stronger LTS as convection is inhibited. This relationship holds for most of the sampling of Fig. 8, but some models show a

negative relationship in the Barbados region. Overall, the figure suggests that the models tend to underestimate sensitivity to inversion characteristics (LTS,  $p_{\text{inv}}$ ) and show widely varying sensitivity to moisture variations ( $\Delta\text{RH}_{700-850}$ ,  $\text{RH}_{850}$ ) that are often of opposite sign to the observations. Many of the models have an unrealistic positive relationship with  $\Delta\text{RH}_{700-850}$ , indicating that stronger convective mixing (smaller negative  $\Delta\text{RH}_{700-850}$ ) is associated with more CC, running counter to the expectation that stronger convective mixing dries the boundary layer and evaporates cloud water (41, 43). Detailed balances cannot be constructed from the available model output, but several plausible reasons exist for models producing unrealistic process balances in shallow cumulus regimes, including coarse resolution (horizontal or vertical) that misses important aspects of the circulation (e.g., mesoscale variability) and the artificial separation of processes (e.g., boundary layer turbulence and cumulus convection), which could create competition among parameterizations and result in erroneous heating and moistening rates.

The range of correlations shown in Fig. 8 assures that some models evince spurious relationships, some of which could be directly associated with cloud feedbacks under climate change. The differing cloud responses under climate change across models is well documented but poorly understood (44). The cloud-controlling factors shown in Fig. 8, along with  $\omega_{500}$ , have been investigated to differing extents with regard to climate change. The shallow convection regimes considered here have received less attention than others, but a few comments can be made. As has been emphasized



here, the trade wind inversion is an important feature of these regimes; it occurs where subsidence warming balances convective and radiative cooling (43, 45), linking it intrinsically to both the large-scale circulation and the small-scale boundary layer mixing. No systematic study of inversion characteristics (in particular,  $p_{\text{inv}}$ ) is available for the CMIP5 archive, but observations support the connection between inversion height and cloud-top height across the subtropical regions (46, 47). More attention has been given to the inversion strength, which is generally inversely related to inversion height. The inversion is expected to strengthen with warming (35, 48), and variations in LTS have been long associated with low-level cloud variations at timescales longer than synoptic variability (32, 49, 50). The change in  $\omega_{500}$  is closely associated with the Hadley circulation response, which is expected to expand under climate change with weaker subtropical subsidence rates (51, 52). The distribution of  $\omega_{500}$  narrows as a consequence, and the regimes considered here become more frequent across the tropics (3). Under equilibrium conditions, energy constraints suggest the near-surface RH should not change much, and climate models show about a 1% increase in trade wind regions (53). Under transient climate change, however, models show decreased lower-tropospheric relative humidity (52, 54). The relative humidity contrast,  $\Delta\text{RH}_{700-850}$ , used here as a measure of shallow convective mixing has not been extensively investigated, but idealized warming experiments tend to suggest an increase (41). These environmental factors interact with each other and with the clouds, making it difficult to draw conclusions about the role of each for cloud feedbacks, but models that incorrectly represent the physics of shallow convection are unlikely to capture the physical mechanisms of the feedback.

## Discussion

Returning to our opening question, have we established whether observations at the BCO are representative of broader tropical regimes? By using monthly means from reanalysis and satellites, we have shown that the Barbados region's clouds are comparable to common cloud regimes across the tropics (Figs. 2 and 3). Barbados undergoes a transition in the large-scale environment from moderate subsidence in the winter to weak convection in the summer, and there are important differences between the seasons that are also found in the broader tropical regimes (Fig. 5). We have intentionally kept the regime definition very broad (using only  $\omega_{500}$ ); doing so produces some discrepancies between the region and the regime, which are instructive for understanding the variation within the regimes but could be reduced with more stringent regime definitions. In particular, the moderate subsidence regime contains more frequent cloudier, geometrically thin low-cloud layers than the Barbados region, which is more often dominated by fields of shallow cumulus.

The similarity between the Barbados region and tropical regimes carries over to the climate models in many ways. In general, the structure of the clouds is similar between the region and regime (Fig. 4), and model biases in cloud properties are also similar. In particular, the underestimate of low-level cloud and the compensating errors in cloud optical properties to achieve a reasonable SWCRE is shared across most of the models (Figs. 6 and 7). Models also frequently exhibit low biases in LTS, particularly under midtropospheric subsidence, and biases in inversion level are generally similar between the region and regime. The linear relationships between  $\text{CC}_{\text{LO}}$  and environmental parameters also tend to be similar between the Barbados region and the dynamical regimes, especially for measures of humidity mixing (Fig. 8).

These similarities suggest that detailed model evaluations using BCO observations could elucidate process-level errors in models and inform model development with impacts across the tropics. Although seemingly self-evident, there are few examples that demonstrate that a long-term observational site is representative of broader regimes (1). It is also worth noting that the methodological approach taken here, comparison between an observational

site and similar dynamical regimes, is directly applicable to other long-term observing sites. A recent study, for example, applied a conceptually similar cloud regime method to a region around the Azores, upstream from Barbados (2).

The comparisons presented have also highlighted some errors in trade wind clouds in climate models. As discussed above, some of the models have substantial errors in the regional circulation near Barbados. Similar errors are undoubtedly present for other regions, and could have important consequences for evaluations of clouds and other phenomena in those regions. A hindcasting approach would be an attractive method to separate errors in the large-scale circulation and those associated with fast, parameterized physics (55, 56). We have also corroborated previous assessments that climate models tend to have too little cloud coverage in the tropics but do not exhibit commensurate errors in CRE, meaning that the simulated low-level clouds are too reflective. The models tend to produce weaker, higher inversions than ERA-Interim. The models also show a great diversity in their representations of the cloud vertical structure (Fig. 4); biases in the cloud vertical structure can point to misrepresentations of the small-scale mixing processes in the lower troposphere, linking the biases in cloud structure to those in boundary layer and inversion characteristics. Observations suggest that cloud variability at Barbados is closely associated with the vertical structure: Cloud near the LCL is rather insensitive to environmental variations, whereas cloud near the inversion is much more variable (57). Many climate models have difficulty distinguishing these layers, and likely do not represent their coupling correctly (12). Much of the variability occurs at timescales of a few days or less (57), so monthly means are unlikely to expose such variability, and, in fact, we find that estimates of CF at these levels have similar variability and are weakly coupled (Tables S1 and S2).

These errors in cloud vertical structure and connections between clouds and the environment cast some doubt on the veracity of climate projections and estimates of cloud feedback. Recent studies have pointed out that inversion strength and SST can be combined to understand low-level CC responses to a changing climate (35), but most such studies have been more focused on stratocumulus regions than on shallow cumulus ones. In the former, the balance of processes is likely to remain relatively similar to the present climate because, even under significant climate change, the quasi-permanent stratocumulus decks will exist over relatively cool water and under relatively strong inversions. Across much of the tropical oceans, however, the SST is warmer, the inversion is weaker, and the boundary layer is more convective. This type of environment, including everything from the weakly convective to moderately subsiding regimes considered here, poses a somewhat different challenge to parameterized physics suites in that there is a delicate balance and interplay between the boundary layer turbulence and shallow convective mixing. These are usually separate parameterizations in climate models, and the cloud feedback in any particular model is linked to which process is dominant (or if the dominant process changes under climate change) (58, 59). As has been described here, the models can achieve some fairly realistic representations of the current climate, but with compensating errors and biases in structure and relative susceptibility to the environment. As the forcing to the system changes, it is not clear if these compensating errors and processes will persist or change. To the extent possible, therefore, these model errors need to be ameliorated to achieve a credible representation of the trade wind regions and increase confidence in climate projections.

**ACKNOWLEDGMENTS.** We acknowledge the World Climate Research Programme's Working Group on Coupled Modelling, and we thank the climate modeling groups (listed in Table S1) for their model output. The ERA-Interim reanalysis was obtained as monthly mean Grib files stored at NCAR [60]. This research was supported by the Regional and Global Climate Modeling Program of the US Department of Energy's Office of Science, Cooperative Agreement DE-FC02-97ER62402.



1. Jakob C, Tselioudis G (2003) Objective identification of cloud regimes in the tropical western Pacific. *Geophys Res Lett* 30(21):2082.
2. Rémillard J, Tselioudis G (2015) Cloud regime variability over the Azores and its application to climate model evaluation. *J Clim* 28(24):9707–9720.
3. Medeiros B, Stevens B, Bony S (2015) Using aquaplanets to understand the robust responses of comprehensive climate models to forcing. *Clim Dyn* 44(7–8):1957–1977.
4. Bony S, Dufresne JL (2005) Marine boundary layer clouds at the heart of tropical cloud feedback uncertainties in climate models. *Geophys Res Lett* 32(20):L20806.
5. von Salzen K, McFarlane NA, Lazare M (2005) The role of shallow convection in the water and energy cycles of the atmosphere. *Clim Dyn* 25(7):671–688.
6. Medeiros B, Nuijens L, Antoniazzi C, Stevens B (2010) Low-latitude boundary layer clouds as seen by CALIPSO. *J Geophys Res* 115(D23):D23207.
7. Wood R, et al. (2015) Clouds, aerosols, and precipitation in the marine boundary layer: An arm mobile facility deployment. *Bull Am Meteorol Soc* 96(3):419–440.
8. Stevens B, et al. (2015) The Barbados Cloud Observatory – Anchoring investigations of clouds and circulation on the edge of the ITCZ. *Bull Am Meteorol Soc*, in press.
9. Klein SA, et al. (2013) Are climate model simulations of clouds improving? An evaluation using the ISCCP simulator. *J Geophys Res* 118(3):1329–1342.
10. Su H, et al. (2013) Diagnosis of regime-dependent cloud simulation errors in CMIP5 models using “A-train” satellite observations and reanalysis data. *J Geophys Res* 118(7):2762–2780.
11. Nam C, Bony S, Dufresne JL, Chepfer H (2012) The ‘too few, too bright’ tropical low-cloud problem in CMIP5 models. *Geophys Res Lett* 39(21):L21801.
12. Nuijens L, Medeiros B, Sandu I, Ahlgrimm M (2015) Observed and modeled patterns of covariability between low-level cloudiness and the structure of the trade-wind layer. *J Adv Model Earth Syst* 7(4):1741–1764.
13. Loeb NG, et al. (2009) Toward optimal closure of the Earth’s top-of-atmosphere radiation budget. *J Clim* 22(3):748–766.
14. Dee DP, et al. (2011) The ERA-Interim reanalysis: Configuration and performance of the data assimilation system. *Q J R Meteorol Soc* 137(656):553–597.
15. Kiehl JT (1994) On the observed near cancellation between longwave and shortwave cloud forcing in tropical regions. *J Clim* 7(4):559–565.
16. Bony S, Dufresne JL, Treut HL, Morcrette JJ, Senior C (2004) On dynamic and thermodynamic components of cloud changes. *Clim Dyn* 22(2):71–86.
17. Rossow WB, Schiffer RA (1999) Advances in understanding clouds from ISCCP. *Bull Am Meteorol Soc* 80(11):2261–2287.
18. Takayabu YN, Shige S, Tao WK, Hirota N (2010) Shallow and deep latent heating modes over tropical oceans observed with TRMM PR spectral latent heating data. *J Clim* 23(8):2030–2046.
19. Hartmann DL, Short DA (1980) On the use of Earth radiation budget statistics for studies of clouds and climate. *J Atmos Sci* 37(6):1233–1250.
20. Ramanathan V, et al. (1989) Cloud-radiative forcing and climate: Results from the Earth Radiation Budget Experiment. *Science* 243(4887):57–63.
21. Brueck M, Nuijens L, Stevens B (2014) On the seasonal and synoptic time-scale variability of the North Atlantic trade wind region and its low-level clouds. *J Atmos Sci* 72(4):1428–1446.
22. Chepfer H, et al. (2010) The GCM-Oriented CALIPSO cloud product (CALIPSO-GOCCP). *J Geophys Res* 115(D4):D00H16.
23. Schwartz MC, Mace GG (2010) Co-occurrence statistics of tropical tropopause layer cirrus with lower cloud layers as derived from Cloudsat and CALIPSO data. *J Geophys Res* 115(D20):D20215.
24. Nuijens L, Medeiros B, Sandu I, Ahlgrimm M (2015) The behavior of trade-wind cloudiness in observations and models: The major cloud components and their variability. *J Adv Model Earth Syst* 7(2):600–616.
25. Medeiros B, Stevens B (2011) Revealing differences in GCM representations of low clouds. *Clim Dyn* 36(1):385–399.
26. Williams K, Ringer M, Senior C (2003) Evaluating the cloud response to climate change and current climate variability. *Clim Dyn* 20(7–8):705–721.
27. Martin ER, Schumacher C (2011) The Caribbean low-level jet and its relationship with precipitation in IPCC AR4 models. *J Clim* 24(22):5935–5950.
28. Liu H, Wang C, Lee SK, Enfield D (2013) Atlantic warm pool variability in the CMIP5 simulations. *J Clim* 26(15):5315–5336.
29. Bodas-Salcedo A, et al. (2011) COSP: Satellite simulation software for model assessment. *Bull Am Meteorol Soc* 92(8):1023–1043.
30. Brient F, et al. (2015) Shallowness of tropical low clouds as a predictor of climate models’ response to warming. *Clim Dyn*, in press.
31. Hartmann DL, Larson K (2002) An important constraint on tropical cloud - climate feedback. *Geophys Res Lett* 29(20):1951.
32. Klein SA, Hartmann DL (1993) The seasonal cycle of low stratiform clouds. *J Clim* 6(8):1587–1606.
33. Klein SA (1997) Synoptic variability of low-cloud properties and meteorological parameters in the subtropical trade wind boundary layer. *J Clim* 10(8):2018–2039.
34. Myers TA, Norris JR (2013) Observational evidence that enhanced subsidence reduces subtropical marine boundary layer cloudiness. *J Clim* 26(19):7507–7524.
35. Qu X, Hall A, Klein S, Caldwell P (2014) On the spread of changes in marine low cloud cover in climate model simulations of the 21st century. *Clim Dyn* 42(9–10):2603–2626.
36. Myers TA, Norris JR (2015) On the relationships between subtropical clouds and meteorology in observations and CMIP3 and CMIP5 models. *J Clim* 28(8):2945–2967.
37. Wood R (2012) Stratocumulus clouds. *Mon Weather Rev* 140(8):2373–2423.
38. Siebesma AP (1998) Shallow convection. *Buoyant Convection in Geophysical Flows*, eds Plate EJ, Fedorovich EE, Viegas DX, Wyngaard JC (Kluwer Acad, Dordrecht, The Netherlands), Vol 513, pp 441–486.
39. Stevens B (2005) Atmospheric moist convection. *Annu Rev Earth Planet Sci* 33(1):605–643.
40. Nuijens L, Stevens B (2012) The influence of wind speed on shallow marine cumulus convection. *J Atmos Sci* 69(1):168–184.
41. Sherwood SC, Bony S, Dufresne JL (2014) Spread in model climate sensitivity traced to atmospheric convective mixing. *Nature* 505(7481):37–42.
42. Kalmus P, Lebock M, Teixeira J (2014) Observational boundary layer energy and water budgets of the stratocumulus-to-cumulus transition. *J Clim* 27(24):9155–9170.
43. Betts AK (1973) Non-precipitating cumulus convection and its parameterization. *Q J R Meteorol Soc* 99(419):178–196.
44. Zelinka MD, et al. (2013) Contributions of different cloud types to feedbacks and rapid adjustments in CMIP5. *J Clim* 26(14):5007–5027.
45. Albrecht BA, Betts AK, Schubert WH, Cox SK (1979) A model of the thermodynamic structure of the trade-wind boundary layer. Part I: Theoretical formulation and sensitivity tests. *J Atmos Sci* 36:90–98.
46. von Engel A, Teixeira J, Wickert J, Buehler SA (2005) Using CHAMP radio occultation data to determine the top altitude of the planetary boundary layer. *Geophys Res Lett* 32(6):L06815.
47. Karlsson J, Svensson G, Cardoso S, Teixeira J, Paradise S (2010) Subtropical cloud-regime transitions: Boundary layer depth and cloud-top height evolution in models and observations. *J Appl Meteorol Climatol* 49(9):1845–1858.
48. Webb MJ, Lambert FH, Gregory JM (2012) Origins of differences in climate sensitivity, forcing and feedback in climate models. *Clim Dyn* 40(3):677–707.
49. Clement AC, Burgman R, Norris JR (2009) Observational and model evidence for positive low-level cloud feedback. *Science* 325(5939):460–464.
50. Zhang Y, Stevens B, Medeiros B, Ghil M (2009) Low-cloud fraction, lower-tropospheric stability, and large-scale divergence. *J Clim* 22(18):4827–4844.
51. Lu J, Vecchi GA, Reichler T (2007) Expansion of the Hadley cell under global warming. *Geophys Res Lett* 34(6):L06805.
52. Lau WKM, Kim KM (2015) Robust Hadley Circulation changes and increasing global dryness due to CO<sub>2</sub> warming from CMIP5 model projections. *Proc Natl Acad Sci USA* 112(12):3630–3635.
53. Laïné A, Nakamura H, Nishii K, Miyasaka T (2014) A diagnostic study of future evaporation changes projected in CMIP5 climate models. *Clim Dyn* 42(9):2745–2761.
54. Sherwood SC, et al. (2010) Relative humidity changes in a warmer climate. *J Geophys Res* 115(D9):D09104.
55. Phillips TJ, et al. (2004) Evaluating parameterizations in general circulation models: Climate simulation meets weather prediction. *Bull Am Meteorol Soc* 85(12):1903–1915.
56. Williams KD, et al. (2013) The Transpose-AMIP II experiment and its application to the understanding of Southern Ocean cloud biases in climate models. *J Clim* 26(10):3258–3274.
57. Nuijens L, Serikov I, Hirsch L, Lonitz K, Stevens B (2014) The distribution and variability of low-level cloud in the North Atlantic trades. *Q J R Meteorol Soc* 140(684):2364–2374.
58. Zhang M, et al. (2013) CGILS: Results from the first phase of an international project to understand the physical mechanisms of low cloud feedbacks in single column models. *J Adv Model Earth Syst* 5(4):826–842.
59. Bretherton CS (2015) Insights into low-latitude cloud feedbacks from high-resolution models. *Philos Trans R Soc Lond A* 373(2054):20140415.
60. European Centre for Medium-Range Weather Forecasts (2012) ERA-Interim Project, Monthly Means. Available at [rda.ucar.edu/datasets/ds627.1/](http://rda.ucar.edu/datasets/ds627.1/). Accessed May 5, 2016.
61. Faller AJ (1981) An average correlation coefficient. *J Appl Meteorol* 20(2):203–205.
62. Marchand R, Ackerman T, Smyth M, Rossow WB (2010) A review of cloud top height and optical depth histograms from MISR, ISCCP, and MODIS. *J Geophys Res* 115(D16):D16206.
63. Pincus R, Platnick S, Ackerman SA, Hemler RS, Hofmann RJP (2012) Reconciling simulated and observed views of clouds: MODIS, ISCCP, and the limits of instrument simulators. *J Clim* 25(13):4699–4720.